



## Dynamic reference electrode for investigation of fluoride melts containing beryllium difluoride

Valery K. Afonichkin<sup>a,\*</sup>, Andrey L. Bovet<sup>a</sup>, Victor V. Ignatiev<sup>c</sup>, Alexander V. Panov<sup>b</sup>, Vladimir G. Subbotin<sup>b</sup>, Alexander I. Surenkov<sup>c</sup>, Andrey D. Toropov<sup>b</sup>, Aleksey L. Zhrebtsov<sup>b</sup>

<sup>a</sup> Institute of High-Temperature Electrochemistry, Russian Academy of Sciences, Ural Branch, 20 Akademicheskaya St., Yekaterinburg 620219, Russia

<sup>b</sup> Russian Federal Nuclear Center All-Russian Scientific Research Institute of Technical Physics, Box 245, Snezhinsk 456770, Chelyabinsk Region, Russia

<sup>c</sup> Russian Research Center Kurchatov Institute, 1 Kurchatov Square, Moscow 123182, Russia

### ARTICLE INFO

#### Article history:

Received 27 February 2008

Received in revised form 6 June 2008

Accepted 15 July 2008

Available online 30 July 2008

#### Keywords:

Molten salt fluorides

Beryllium reference electrode

Redox potential

### ABSTRACT

Existing designs of reference electrodes for potentiometric measurements in fluoride melts do not meet basic requirements of the long exposure corrosion tests to be performed. A new diaphragm-free three-electrode meter with a nonstationary (dynamic) beryllium reference electrode for the redox potential measurements was developed. Optimum conditions of forming dynamic beryllium reference electrode were determined in the laboratory tests in isothermal cell. The device for redox potential measurement was designed and it was shown that it is highly sensitive to changes redox potential within  $\pm 5$  mV. Reliability and efficiency of diaphragm-free device with dynamic reference electrode was confirmed in the thermal convection corrosion loop operating more than 1200 h with molten 15LiF–58NaF–27BeF<sub>2</sub> mixture (mol%) at a maximum temperature of about 700 °C.

© 2008 Elsevier B.V. All rights reserved.

### 1. Introduction

Recent years have demonstrated revisiting of interest in nuclear energy systems employing technology of molten salt fluorides for

- consumption of transuranic elements while extracting their energy;
- electricity production in Th–U breeder cycle;
- coolant application in solid fuel fast reactor designs;
- pyrochemical reprocessing of advanced fuels;
- high temperature process heat applications, e.g., hydrogen production;
- production of isotopes for medical needs.

For the control of the composition and the purity of the molten salt streams, in-line and reliable analytical techniques will be required [1]. One of the most important parameters to monitor and control is the redox potential of the salt because it influences the chemical and, perhaps, some physical properties of the salt. Particularly it determines the solubility of various fission products and actinides in the melt and the corrosiveness of the molten salt with respect to structural materials. Changes in the redox potential

provide an indicator of off-operation of molten salt clean up systems or a leak in the system with air or other fluids entering the salt.

The objective of this work was to develop reference electrode (RE) for in-line accurate measurements (with an error not more than  $\pm 5$  mV) of redox potential of fluoride melt in the long exposure corrosion tests (>1000 h).

Analysis of the literature has shown that more often for such aims various modifications of classic emf method are used (Fig. 1). This method has high sensitivity to the change of redox potential of the system, simple in apparatus performance and provides good reproducibility of results [2–4].

According to the literature data, the continuous operation time of such potentiometric devices did not exceed 100 h. Moreover, the studies were performed under isothermal conditions or the stepwise temperature changes, while the RE half-element was in equilibrium with a small volume of the fluoride salt melt for the most part of the experiment. Long exposure tests of such devices in thermal convection loops have not been reported in the literature.

### 2. Results and discussion

#### 2.1. Selection of the RE design

The set of requirements imposed on the design and operation of the device for redox potential measurement (DRPM) shows that

\* Corresponding author. Tel.: +7 343 362 3066; fax: +7 343 374 5992.

E-mail address: [afonichkin@ihte.uran.ru](mailto:afonichkin@ihte.uran.ru) (V.K. Afonichkin).

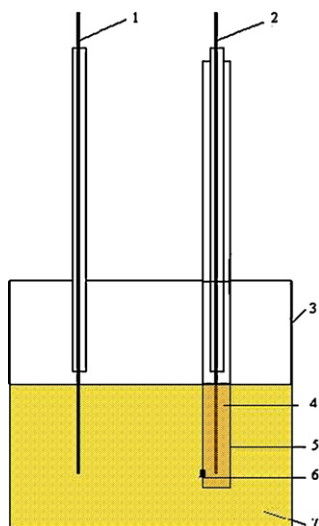


**Fig. 1.** Design of the ion transfer-free galvanic cell for the redox potential measurement: (1) indicator electrode; (2) reference electrode; (3) crucible; (4) standard electrolyte; (5) porous ampoule with diaphragm (6) or without diaphragm; and (7) test electrolyte.

the transfer-free galvanic elements (Fig. 1) studied earlier, cannot guarantee the stable operation within required time in corrosion loop. The specific features of experiments in thermal convection corrosion loop are the following:

- a big enough volume of the fluoride melt in system ( $>1$  l);
- a nonequilibrium of the system, caused by difference in molten salt temperature (up to  $100$  °C) between cold and hot legs of the loop;
- significant salt flow velocity (from  $0.01$  up to  $10$  cm  $s^{-1}$ ) in system.

All these lead to a high rate of the interaction between the membrane material and the fluoride melt, to mass transfer of additional corrosion products in the system, and as result to membrane destruction. Therefore, DRPM's based on transfer-free galvanic elements were avoid from the further consideration.

Particular case of galvanic element with ion transfer (Fig. 2) for melts containing beryllium difluoride is RE of pure metallic

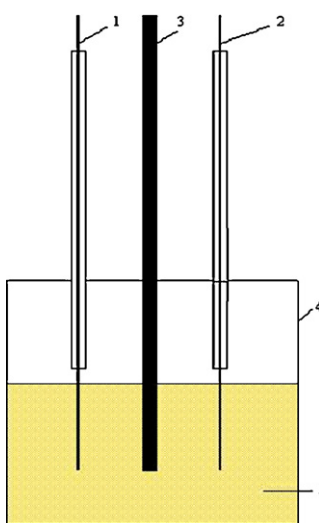


**Fig. 2.** Design of the galvanic cell with ion transfer for the redox potential measurement: (1) indicator electrode; (2) dynamic reference electrode (cathode); (3) glassy-carbon anode; (4) crucible; and (5) molten salt electrolyte.

beryllium, which in these conditions, takes stationary (quasi-equilibrium) potential close to equilibrium. Practical use of such RE is impeded by relatively high chemical activity and electronegativity of beryllium in the melts under study [5], and this leads to deposition of electropositive admixtures on beryllium surface and uncontrolled shift of its potential into positive region. These phenomena can be minimized using dynamic RE. Behavior of different dynamic electrodes was explored earlier both in chloride [6], and in fluoride salt melts [7,8]. Its feature consists of the fact that electrode preserves constant value of potential within limited interval of time and is formed before each measurement of redox potential of the system under study by passing short-time pulse of direct current between two conductors semi-immersed in the melt. One of them is the cathode, on which a beryllium deposit is formed. This beryllium is reversible to ions  $Be^{2+}$  of electrolyte, and after disconnecting of polarizing current it is used as RE. Another electrode (anode) plays supporting function. After rupture of polarizing chain, there is relaxation of cathode potential (returning to initial value) and registration of the emf change vs. time in cell consisting of nonpolarized indicator electrode and cathode. On the curve emf vs. time, one observes more or less long horizontal plateau corresponding to constant quasi-equilibrium melt redox potential measured relatively to beryllium RE, but with inverse sign.

This type of dynamic RE is attractive first of all by the fact that under current impact, microscopic amount of potential-determining metal is deposited on the cathode surface. The time of existence of such electrode is selected experimentally and usually does not exceed several minutes. That is why its impact on the system redox potential is negligible. There is no sufficient change of electrodeposited beryllium activity in its surface layer, that is why the shift of dynamic electrode potential during experiment is not expected even at the presence of certain concentration of electropositive admixtures in the melt, due to low coefficients of diffusion of doped ions in fluoride melts ( $D \approx 10^{-6}$  cm $^2$   $s^{-1}$ ) [9]. Although starting materials of high purity were used in the production of fused fluoride further purification was needed before the salts were used in loop system. Two steps were required: one for removal of oxides and other to decrease concentration of metallic fluorides. Last ones primarily include nickel, iron and chromium ions.

Co-deposition of admixtures during formation of dynamic electrode can be limited using high densities of electrolysis current. Increase of current pulse amplitude will lead to deposition of purer product, as far as in the regime of limited diffusion current, admixtures are reduced on cathode with constant rates, and beryllium ions flow at their high concentration in a melt and ratio  $[Be^0]/[Be^0 + admixtures\ sum]$  in cathode deposit can be varied in wide ranges.

## 2.2. Selection of electrode materials

In order to build DRPM with optimum operating characteristics, it is necessary to correctly select materials for fabrication of indicator electrode, cathode, on which beryllium is deposited, and auxiliary electrode (anode).

A wire or rod, semi-immersed in the melt, usually serves as the indicator electrode. Its material is indifferent to all salt mixture constituents over a broad interval of redox potentials. This means that the electrode material should possess a high-corrosion resistance in the melt and should not participate in exchange, redox or electrochemical reactions with main salt mixture constituents, corrosion products and cover gas. The choice of such materials is limited. Therefore, noble (platinum and gold) or most electropositive and, generally, refractory (tungsten, molybdenum

and rhenium) metals, and also carbon materials, e.g., glassy-carbon, are used for this purpose. Considering the requirements on the mechanical strength and availability of the electrode material, we have selected a molybdenum wire.

Material of auxiliary electrode should satisfy all the requirements imposed on the indicator electrode material. However, the main requirement is its stability during anodic polarization in the melt. It is not advisable to use metals as the material of the anode, because each DC pulse, needed to form the dynamic beryllium electrode, will lead to metal ionization on the anode. This process causes accumulation of electropositive impurities in the melt. Nonconsumable anodes made of oxide, nitride or other materials with anion conductivity cannot be used either, because these species have relatively high solubility in fluoride melts and release  $O^{2-}$  and  $N^{3-}$  impurity anions, etc., to the melt during anodic polarization. Carbon materials (graphite, glassy-carbon, and others) are single but not an ideal alternative either. Anodic polarization of carbon electrodes is accompanied by oxidation of  $F^-$  ions. The final product of this reaction is a mixture of gaseous freons, which may cause blocking of the electrode surface and lead to the “anodic effect” at a high-current density. When a large quantity of electricity passes in the electrochemical cell, such electrode may burn out, leading to the break in the electric circuit and failure of the DRPM.

Taking into account that materials, which would be stable during anodic polarization in fluoride salt melts and would not

release impurity ions to the melt, are unavailable in the nature, we decided to use a glassy-carbon rod as the auxiliary electrode. Only gaseous freons, which do not affect the melt composition and the redox potential of the system as a whole, are formed during operation of this electrode.

During the experiment cathode operates in three different modes:

- cathodic formation of the dynamic beryllium RE;
- measurement of the emf between the indicator electrode and cathode;
- relaxation of the cathode potential and idling.

In the first mode, the selected material of the cathode should be coated with metallic beryllium and should not form liquid alloys with the potential-controlling component having a low activity. If low-melting eutectics is formed between beryllium and the cathode material, the thermodynamic activity of beryllium, which may be present as a solution and a solid intermetallide in the liquid surface layer of the electrode or form separate crystals on the surface of the liquid alloy, becomes uncertain. Stability and reproducibility of the potential of this liquid-film dynamic RE will mainly depend on the invariance of the current pulse characteristics, but the time required for spontaneous dissolution of the surface layer and the reset of the cathode potential, may exceed the permissible limit. The presence of a continuous series of solid

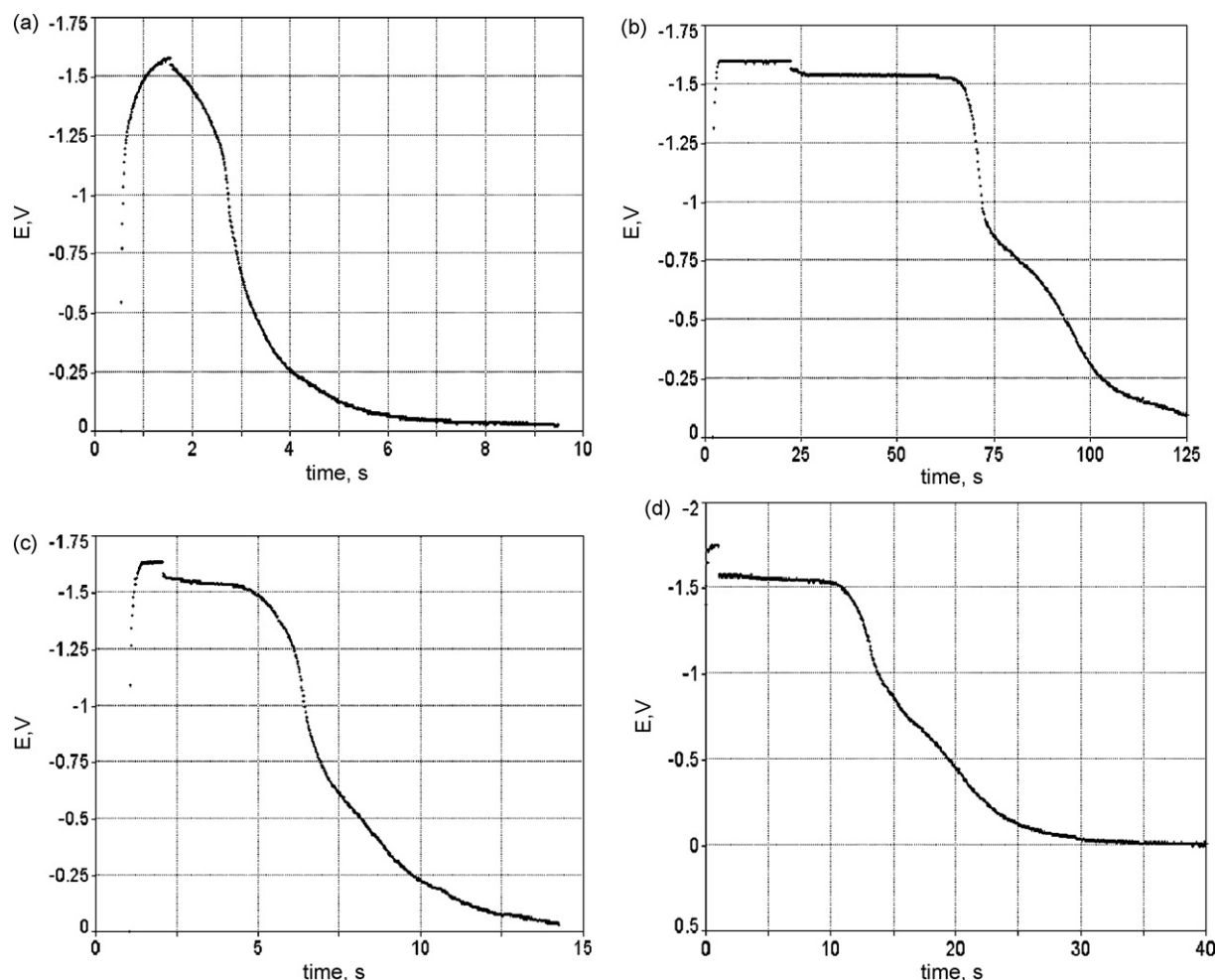


Fig. 3. Effect of DRPM polarization conditions on the emf relaxation curves at 600 °C: (a)  $I = 20$  mA,  $\tau = 1$  s; (b)  $I = 20$  mA,  $\tau = 20$  s; (c)  $I = 40$  mA,  $\tau = 1$  s; and (d)  $I = 100$  mA;  $\tau = 1$  s.

solutions between beryllium and the cathode material in the region of the phase equilibrium diagram adjacent to pure beryllium is unwanted either. After a short-time polarization, the curve of the cathode potential decay may not exhibit a clear-cut plateau, which is necessary for an accurate determination of the emf of the galvanic element made up of the indicator electrode and the dynamic beryllium electrode.

One of the most important thermodynamic characteristics in selection of the cathode material is the standard electrode potential of the metal in test melt. This potential must be more positive than standard potentials of impurity metals (Ni, Fe and Cr) whose ions pass to the melt because the samples under study become corroded during long-time corrosion tests. It is only under this condition that ions of impurity metals will not oxidize the cathode during long idling and will not be reduced on it, changing the composition and the area of the surface layer. Unfortunately, metals, which would not form alloys with beryllium and would be indifferent to nickel ions are not available.

As the result of phase diagrams analysis for binary systems [10] and taking into account mentioned above considerations, a molybdenum wire was selected as cathode material.

Fabricated DRPM was tested in the melt with eutectic 15LiF–58NaF–27BeF<sub>2</sub> mixture (in mol%), whose components were dried beforehand by a standard method. A powder mixture of fluorides was melted in a glassy-carbon crucible and then zone melting was performed three times in pure argon using a molybdenum boat.

The experiment in test cell at  $600 \pm 3$  °C included two stages. A molybdenum wire cathode 1 mm in diameter was immersed into the melt to a depth of 3 mm. The first stage was concerned with the influence of the polarization current (10–500 mA) and the pulse duration (1–200 s) on the emf relaxation curves between the dynamic beryllium electrode and the indicator electrode. It was found that the relaxation curves exhibit several waves, which correspond to dissolution of alloys and intermetallic compounds of beryllium, molybdenum, and admixture metals at potentials more positive than the beryllium potential. The location, the shape, and the extent of the waves depend on the cathode polarization conditions, but generally they do not interfere with measurements of the melt redox potential relative to the dynamic beryllium RE.

As can be seen from Fig. 3, short current pulses (1 s) of a small amplitude did not provide a beryllium deposit on the cathode and the plateau of the beryllium dissolution in the emf relaxation curve was either absent (curve a) or its extent was too small (curve c) for accurate measurement of the salt redox potential. As the cathode polarization time was increased (curve b), more beryllium was deposited and the emf relaxation curves had a pronounced horizontal section several seconds or tens of seconds long.

The measurement error of the redox potential was a minimum under these conditions of the DRPM polarization. A high-current density caused appearance of one more wave in the relaxation curve (curve d) before the beryllium plateau. The wave was due probably to formation of a dilute beryllium–sodium alloy on the cathode surface. This by process could cause a considerable error in the measured redox potential. Therefore, a polarization current  $I = 10\text{--}100$  mA and current pulses  $\tau = 10\text{--}50$  s were used in later experiments. As a result, it was possible to decrease the effect of the electric current on the test system, shorten the relaxation time of the measured emf, and diminish the contamination of the cathode surface with electropositive impurity elements, which were reduced on the cathode at electrolysis. Depending on the cathode polarization conditions (the current, the pulse duration, the melt temperature, and the concentration of impurities interacting with beryllium), the extent of the horizontal section can change considerably. The measurement accuracy of the redox potential after each cathode polarization was within  $\pm 1$  mV. The

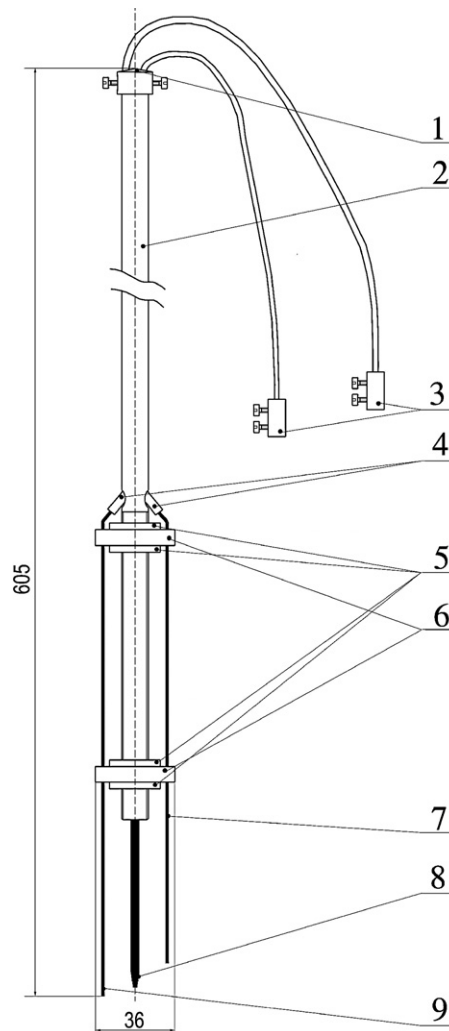


**Fig. 4.** DRPM design: (1) epoxy compound; (2) central tube; (3) current leads; (4) insulating ceramic sleeve; (5) nuts; (6) insulating plates made of boron nitride; (7) indicator electrode; (8) anode and (9) cathode.

given maximal error margins for the redox potential ( $\pm 5$  mV) refer to the reproducibility of the redox potential values in a series of consecutive measurements made in one and the same melt at one and the same temperature ( $T = 600$  °C) during 24 h.

Sensitivity of the DRPM to changes in the redox potential of the melt was checked at the second stage. To shift the potential to the negative side, an additional molybdenum electrode was fitted in the cell and several dozens of milligrams of beryllium were deposited on this electrode using a glassy-carbon anode. After the electrolysis procedure was complete, the cathodic deposit of

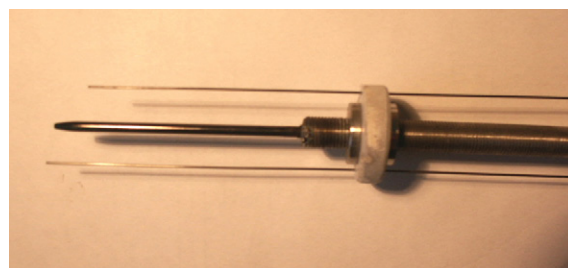


**Fig. 5.** The external appearance of the bottom (working) part of the DRPM.

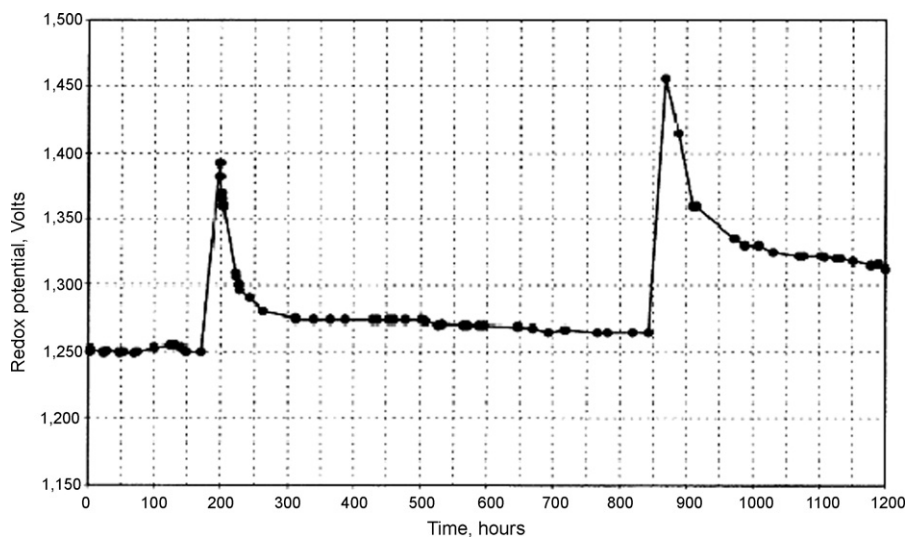


Fig. 6. The redox potential vs. time measured by DRPM in the thermal convection loop.

beryllium was held in contact with the melt for half an hour and then was removed to the gas space of the cell. The subsequent measurements of the redox potential of the indicator electrode showed that after the electrolyte was reduced with beryllium, the equilibrium potential of the system shifted to the negative side for about 100 mV and then remained almost constant for 5 h.

In order to perform long exposure corrosion tests in thermal convection loop, DRPM was fabricated, whose design is described below. The central part of the device (Fig. 4), providing necessary strength and rigidity of the design, is a tube made of stainless steel, which also played the function of current supply to anode. Fixing glassy-carbon rod (anode) is put into the lower end of the tube. Two round boron nitride plates fixed on external surface of the tube perform the function of electrical insulator and limit electrode mobility. Above the upper boron nitride plate, in central tube, there are two shifted apertures for putting cathode and indicator electrode inside the tube. Electrical insulation of wire electrodes from internal wall of the central tube is made with the help of ceramic tubes put on each electrode. The impermeability of electrode output from central tube is achieved by using composition based on epoxy resin.

The developed diaphragm-free device with dynamic reference electrode (Fig. 5) was tested at temperatures up to 700 °C in thermal convection loop constructed of Ni-based alloy NP2 and filled by 15LiF–58NaF–27BeF<sub>2</sub> melt (mol%).

The behavior of this device was somewhat different from the behavior of its laboratory prototype. The major distinction was that the cathode immersion depth ( $H = 3$  mm), which was chosen for the laboratory isothermal cell, proved to be unacceptable for the corrosion loop with the temperature gradient across the salt melt equal to  $\approx 100$  °C. Because of the intensive heat removal via the 1 mm diameter Mo wire, which was streamlined by convective flows of cold argon and the melt whose temperature was lower than that at the bottom of the loop, the surfaces of the cathode and the anode were covered with a hard salt, while the electrical resistance between them increased sharply. It was found experimentally that the setting depth of all the electrodes should be increased to 16–20 mm for the normal operation of the device in the loop. The polarization currents were made higher in proportion to the varying surface of the immersed part of the cathode. Upon these modifications the relaxation curves of the emf between the nonpolarizable Mo indicator electrode and the cathode, which were measured after its short-time polarization, differed little from

the curves measured in laboratory experiments. We did not observe any emf oscillations in the relaxation curves, including the plateau region, which would be due to the flow of the melt at a speed of  $\approx 5$  cm s<sup>-1</sup>. The reproducibility of the redox potential values, which were measured in the loop at regular short intervals ( $\approx 20$  min), was not inferior to the reproducibility achieved in the laboratory experiments.

Loop operated more than 1200 h and we encountered no problems with measurements of the melt redox potential during this period. The redox potential behavior in the course of corrosion test is given in Fig. 6. Peaks in the redox potential, which are clearly seen in the figure, related to contact of the loop internals with laboratory atmosphere when replacing the material specimens under study [11]. After loop sealing, the redox potential gradually returned to its initial value, but remained short of this value because the concentration of the alloy corrosion products increased due to the ingress of oxidizers (water vapor and oxygen) into the system. The redox potential was nearly constant or decreased gradually over the periods before and after the jumps. Results of the measurements are characterized by a small spread of points. All these observations are seen in Fig. 6 and point to the reliability, a long lifetime and a high sensitivity of the DRPM, as well as to the accuracy of the values measured by this meter.

### 3. Conclusions

Analysis of the literature data concerning the use of various reference electrodes for potentiometric measurements in fluoride salt melts showed that the existing designs do not meet basic requirements of the prolonged corrosion tests to be performed on the thermal convection loop.

A new diaphragm-free three-electrode meter with a nonstationary (dynamic) beryllium reference electrode was developed for measurement of the redox potential of the BeF<sub>2</sub> containing salt melt.

Preliminary tests of the laboratory model of the design for measuring the redox potential in 15LiF–58NaF–27BeF<sub>2</sub> salt mixture (in mol%) at 600 °C allowed determining optimal conditions for formation of the dynamic beryllium reference electrode, which ensures reproducibility of the redox potential values of the melt ( $H = 3$  mm,  $I = 10$ –100 mA,  $\tau = 1$ –50 s).

It was shown that the three-electrode DRPM with a dynamic reference electrode is highly sensitive to changes in the redox potential of the melt and measures these changes to within  $\pm 5$  mV.

Results of 1200 h corrosion experiment in the thermal convection with on-line redox potential measurement demonstrated reliability of developed DRPM.

#### Acknowledgment

The generous financial support of this work by the ISTC # 1606 Project is gratefully acknowledged.

#### References

- [1] V. Ignatiev, V. Subbotin, V. Afonichkin, et al. in: Proceedings of GLOBAL 2005, Tsukuba, Japan, October 9–13, 2005, Paper No. 027.
- [2] M.V. Smirnov, *Electrode Potentials in Chloride Melts*, Nauka, Moscow, 1973.
- [3] D.J.G. Ives, G.J. Janz (Eds.), *Reference Electrodes: Theory and Practice*, Academic Press, New York, London, 1961.
- [4] A.F. Alabyshev, M.F. Lantratov, A.G. Morachevski, in: A.F. Alabyshev (Ed.), *Reference Electrodes for Salt Melts*, Metallurgiya, Moscow, 1965.
- [5] C.F. Baes Jr., *Nucl. Metall.* 15 (1969) 615–644.
- [6] Y. Berghoute, A. Salmi, F. Lantelme, *J. Electroanal. Chem.* 365 (1994) 171–177.
- [7] K. Ema, Y. Ito, T. Takenaka, J. Oishi, *Electrochim. Acta* 32 (1987) 1537–1540.
- [8] N. Adhoum, J. Bouteillon, D. Dumas, J.C. Poignet, *J. Electroanal. Chem.* 391 (1995) 63–68.
- [9] D.L. Manning, G. Mamantov, *High Temp. Sci.* 3 (1971) 533–536.
- [10] N.P. Lyakishev (Ed.), *Phase Equilibrium Diagrams of Binary Metal Systems*, Mashinostroyeniye, Moscow, 1996.
- [11] V. Ignatiev, V. Subbotin, V. Afonichkin, et al. *Atom. Energy* 101 (2006) 730–738.